J Fluoresc (2016) 26:155–161
DOI 10.1007/s10895-015-1696-9

ORIGINAL ARTICLE

A Rhodamine-Benzimidazole Based Chemosensor for Fe^{3+} and its Application in Living Cells

Gongchun Li[1] · Jun Tang[2] · Peigang Ding[2] · Yong Ye[2]

Received: 30 July 2015 / Accepted: 14 October 2015 / Published online: 30 October 2015

Abstract A rhodamine-benzimidazole based chemosensor was designed and prepared for Fe^{3+} via opening of the spiro-ring to give fluorescent and colored species. **L** exhibited high selectivity and excellent sensitivity in both absorbance and fluorescence detection of Fe^{3+} in aqueous solution with comparatively wide pH range (5.8–7.4). The detection limit of this newly developed probe was shown to be up to 2.74 μM. The reversibility establishes the potential of both probes as chemosensors for Fe^{3+} detection. Fluorescence imaging experiments of Fe^{3+} in living MGC803 cells demonstrated its value of practical applications in biological systems.

Keywords Rhodamine · Fluorescence · Fe^{3+}

Introduction

Among transition metal ions, iron is the most abundant essential trace element for both plants and animals. It plays an important role in enzyme catalysis, cellular metabolism, DNA, RNA synthesis [1, 2] and as an oxygen carrier in haemoglobin and a cofactor in many enzymatic reactions involved in the mitochondrial respiratory chain [3–6]. Besides the beneficial effects, less iron in the body has been reported linked to diabetes, anemia, liver and kidney damages, and heart diseases [7]. While, deposition of iron in the central nervous system has been involved in a number of diseases, such as Parkinson's and Alzheimer's disease, associated with an increased quantity of iron [8]. Much effort has been focused on the development of fluorescent Fe^{3+} indicators, especially those that exhibit selective Fe^{3+}-amplified emission [9–12].

Fluorescent sensors for metal ions have consistently demonstrated their potential in a variety of fields, such as biological probes, environmental sensors [13–15]. The rhodamine framework is an ideal mode to construct fluorescent chemosensors due to its excellent photophysical properties such as long absorption and emission wavelength, large absorption coefficient and high fluorescence quantum yield [16]. To data, some rhodamine based probes for Fe^{3+} have been reported [17–21], however, an organic cosolvent was needed to guarantee a high probe affinity for Fe^{3+} and there were only a few successful examples of fluorescent probes for detecting Fe^{3+} ions being used in natural water samples for Fe^{3+}.

Herein, a rhodamine-benzimidazole chemosensor was prepared by a new method which is different to Han's [22]. The title compound could sensitively and selectively detect Fe^{3+} in Tris-HCl buffer solution. It also displayed enhanced fluorescence intensities and clear color changes upon recognition. Moreover, fast response (in 10 s) and neutral aqueous medium for Fe^{3+} made it possible to be practical application. The probe could be applied in biological systems for the detection of Fe^{3+} through confocal laser scanning microscopy experiments.

Electronic supplementary material The online version of this article (doi:10.1007/s10895-015-1696-9) contains supplementary material, which is available to authorized users.

✉ Yong Ye
yeyong03@tsinghua.org.cn

[1] School of Chemistry and Chemical Engineering, Xuchang University, Xuchang 461000, China

[2] Phosphorus Chemical Engineering Research Center of Henan Province, The College of Chemistry and Molecular Engineering, Zhengzhou University, Zhengzhou 450052, China

Scheme 1 Synthetic route of target compound

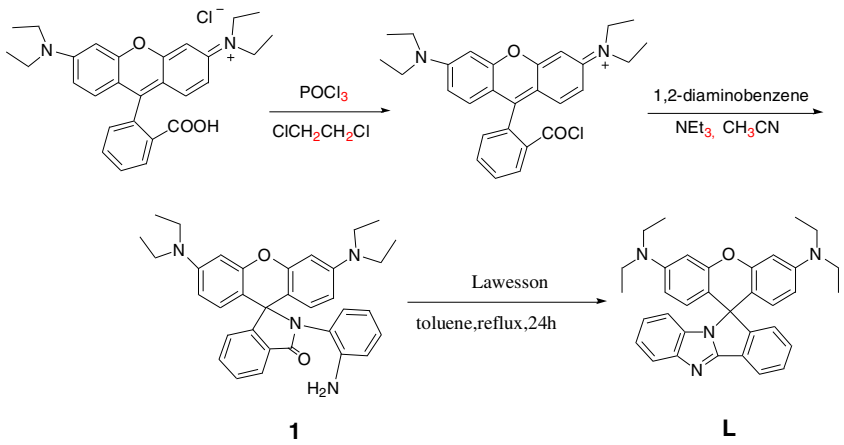

Experimental

Apparatus Reagents and Chemicals

Fluorescence spectra measurements were performed on the F-4500 FL Spectrophotometer, and the excitation and emission wavelength band passes were both set at 5.0 nm. Absorption spectra were measured on a UV-2102 double-beam UV/VIS spectrometer, Perkin Elmer precisely. NMR spectra were recorded on a BrukerDTX-400 spectrometer in $CDCl_3$, using TMS as internal standard. Mass spectral determination was carried on a HPLC Q-T of HR-MS.

All the materials for synthesis were purchased from commercial suppliers and used without further purification. The solutions of metal ions were prepared from their nitrate salts, except for $FeCl_3$, $FeCl_2$, $CrCl_3$, $AlCl_3$ and $MnCl_2$. The metal ions were prepared as 10.00 mM in water solution.

Synthesis

Synthesis of Compound L

As shown in Scheme 1, compound **1** was synthesized according to the literature [23]. The concrete synthesis way of compound **L** was described as follows: Compound **1** (266 mg, 0.5 mmol) and Lawesson's reagent (243 mg, 0.6 mmol) were dissolved in dry toluene, and the reaction mixture was stirred at 110 °C for 24 h under N_2 atmosphere. After removing the solvent under reduced pressure, the residue was purified by

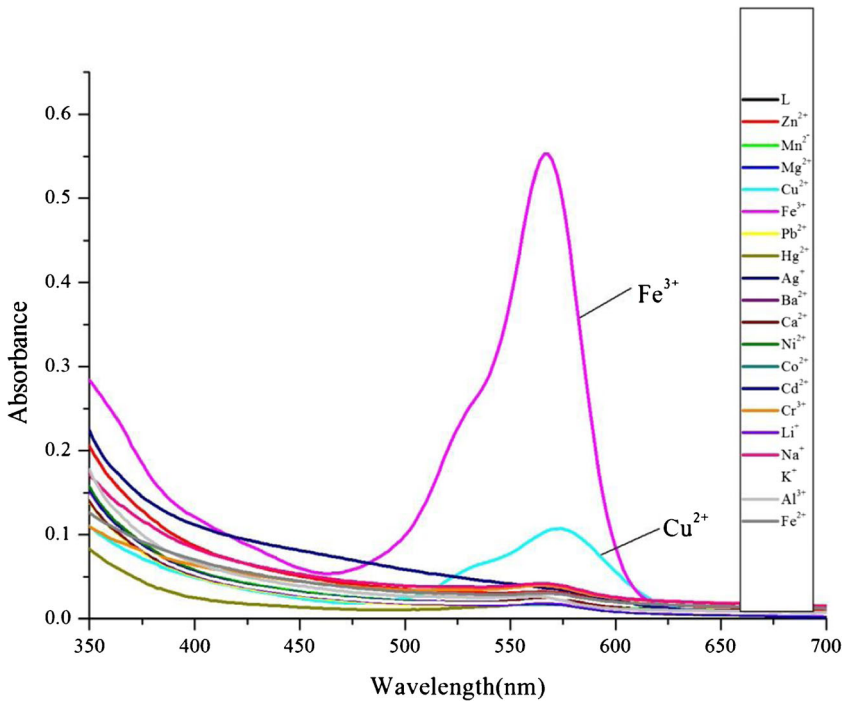

Fig. 1 Absorbance spectra of **L** (10 μM) in Tris-HCl buffer solution (2.5 mM, pH = 7.0) with the presence of 10 equiv. of various species

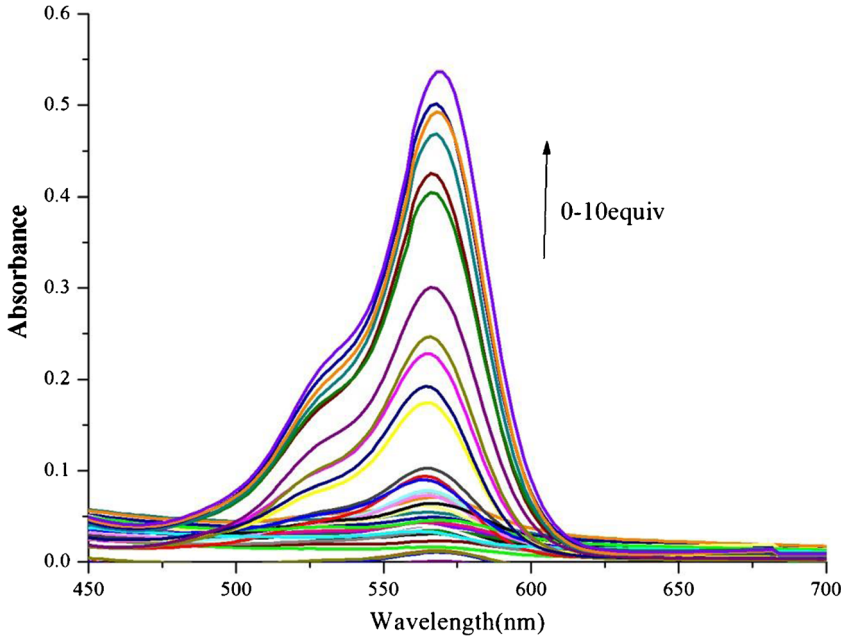

Fig. 2 Absorption spectra of L (10 μM) with gradual addition of various amounts of Fe^{3+} (from bottom 0–10 equiv) in Tris-HCl buffer solution (2.5 mM, pH = 7.0)

column chromatography using EA/PE = 1:1 as eluent to afford **L** (202 mg, 78.6 %).^{1}H-NMR(400 MHz, CDCl3): 1.14 (t, 12 H, *J* = 7 Hz), 3.31 (q, 8 H, *J* = 7 Hz), 6.15 (q, 2 H, *J* = 3.7 Hz), 6.31 (d, 2 H, *J* = 8.8 Hz), 6.49 (d, 2 H, *J* = 2.4 Hz),6,94 (d, 1 H, *J* = 8 Hz), 7.02 (t, 1 H, *J* = 7.4 Hz), 7.16 (t, 1 H, *J* = 7.4 Hz), 7.22 (d, 1 H, *J* = 7.6 Hz), 7.38 (q, 1 H, *J* = 5 Hz), 7.49 (q, 1 H, *J* = 5 Hz), 7.8 (d, 1 H, *J* = 8.4 Hz), 8.09 (s, 1 H). ^{13}C NMR (100 MHz, CDCl3) δ (ppm): 12.6, 44.3, 97.7, 106.2, 108.1, 110.2, 120.0, 121.4, 121.9, 122.5, 124.8, 127.8, 128.3, 128.6, 130.5, 130.9, 148.5, 148.9, 153.0, 156.1, 156.4. HR-MS: $C_{34}H_{35}N_4O$ $[M + H]^+$, calculated for 515.2805. Found: 515.2807. (Supporting Information, Figs. S1–S3).

Results and Analysis

The structure of compounds **L** was characterized by ^{1}H NMR, ^{13}C NMR, and HR-MS. The results were in good agreement with the structure showed in Scheme 1. Fluorescence and

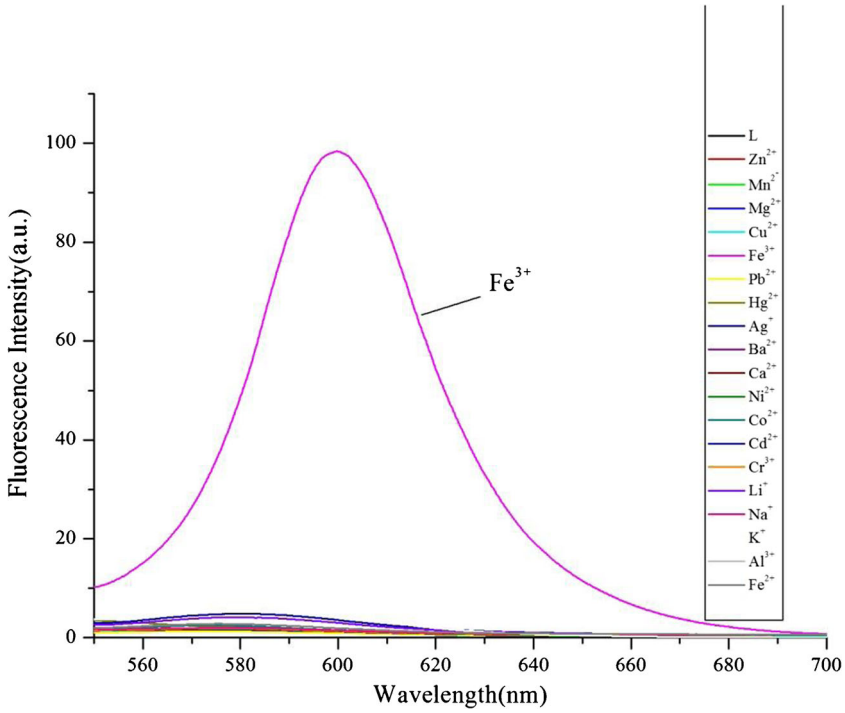

Fig. 3 Fluorescence spectra of **L** (10 μM) in the presence of 100 μM different metal ions in Tris-HCl buffer solution (2.5 mM, pH = 7.0). λ_{ex} = 520 nm, scan range 550–700 nm, slit width 5 nm

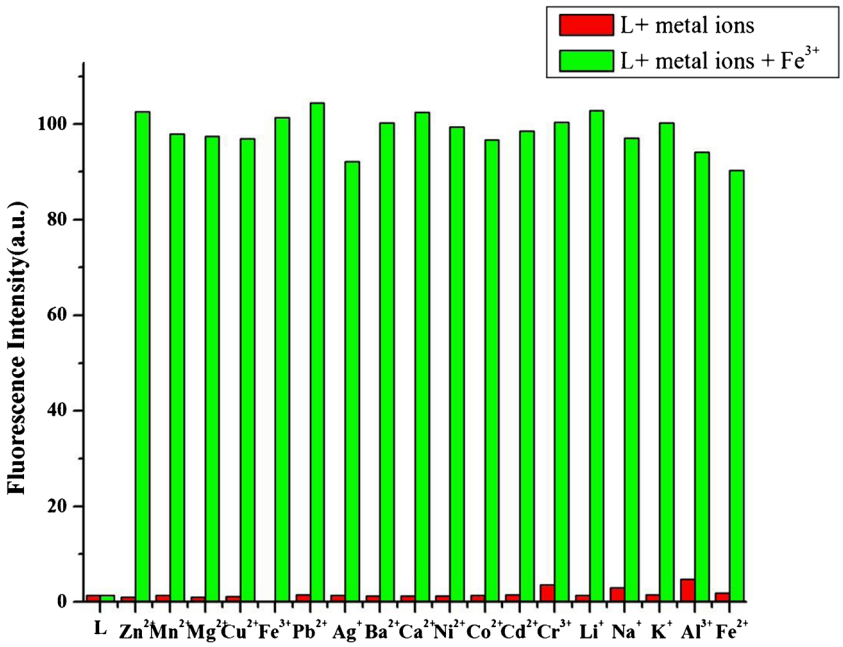

Fig. 4 Fluorescence responses of **L** to various cations in Tris-HCl buffer solution (2.5 mM, pH = 7.0). [**L**] =10 μM, λ_{ex} = 520 nm, λ_{em} = 600 nm

UV–vis studies were performed using a 10 μM solution of **L** in a Tris-HCl (2.5 mM) buffer solution with appropriate amounts of metal ions. Solutions were shaken for 15 min before measuring the absorption and fluorescence in order to make the metal ions chelate with the sensors sufficiently.

UV–vis Spectral Responses of L

As shown in Fig. 1, UV–vis spectrum of compound **L** (10 μM) exhibited only very weak bands over 450 nm. Adding of 10 equiv. Fe^{3+} into solution immediately resulted in a significant enhancement of absorbance at about 554 nm, and simultaneously accompanying with the color changes from colorless to red. Under the identical condition, no obvious response could be observed upon the addition of other ions including Zn^{2+}, Cr^{3+}, Mg^{2+}, Ca^{2+}, Cd^{2+}, Al^{3+}, Pb^{2+}, Hg^{2+}, Ba^{2+}, Ni^{2+}, Fe^{2+}, Mn^{2+}, K^{+}, Li^{+}, Ag^{+}, Co^{2+} and Na^{+} except for Cu^{2+} (Fig. 1), which caused a mild effect compared to Fe^{3+}. The results demonstrated that **L** was characteristic

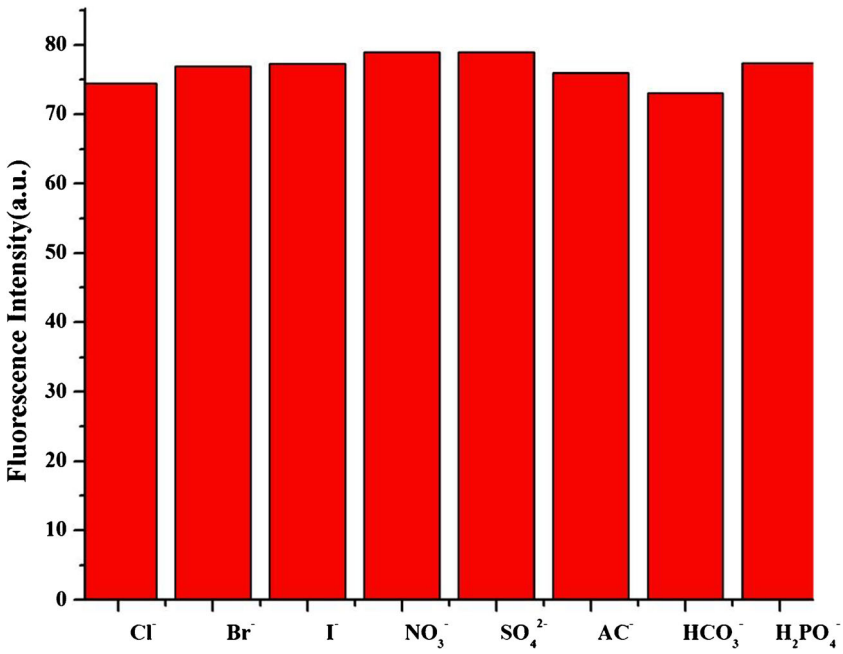

Fig. 5 Fluorescence responses of **L** to various anions in Tris-HCl buffer solution (2.5 mM, pH = 7.0). [**L**] =10 μM, λ_{ex} = 520 nm, λ_{em} = 600 nm

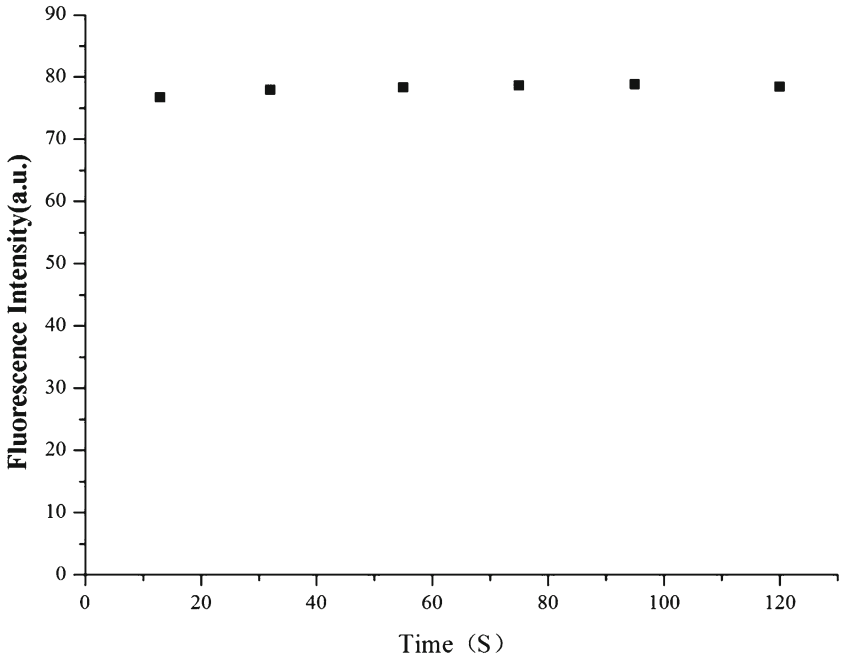

Fig. 6 Effect of reaction time on the fluorescence intensity (at 600 nm) of **L** (10 μM) in the absence and presence of 10 equiv. Fe^{3+} in Tris-HCl buffer solution (2.5 mM, pH = 7.0). (λ_{ex} = 520 nm, slit =5 nm)

of high selectivity toward Fe^{3+} over other competitive metal ions.

To further investigate the interaction of Fe^{3+} and **L**, an ultraviolet titration experiment was carried out (Fig. 2). A linear increasing of absorption intensity of **L** could be observed accompanying with color changes from colorless to red along with the increasing concentrations of Fe^{3+} (Fig. 1, inset). To determine the stoichiometry of the iron–ligand complex, Job's method for absorbance measurement was applied [24] (Fig. S4). The absorbance reached a maximum when the ratio being 0.5, indicating a 1:1 stoichiometry of the Fe^{3+} to **L** in the complex.

Fluorescence Spectral Responses of L

The selectivity of **L** for Fe^{3+} was further observed in the fluorescent spectra. As shown in Fig. 3, **L** exhibited a very weak fluorescence in the absence of metal ions. When 10 equiv. Fe^{3+} was introduced in a 10 uM solution of **L** in Tris-HCl buffer solution (2.5 mM, pH = 7.0), a remarkably enhancement of fluorescence spectra was observed. Competition experiments were carried out to explore the use of **L** as an ion-selective fluorescent probe for Fe^{3+}. **L** (10 uM) was treated with 10 equiv. Fe^{3+} in the presence of other metal ions (10 equiv.). As shown in Fig. 4, the competing metal ions showed

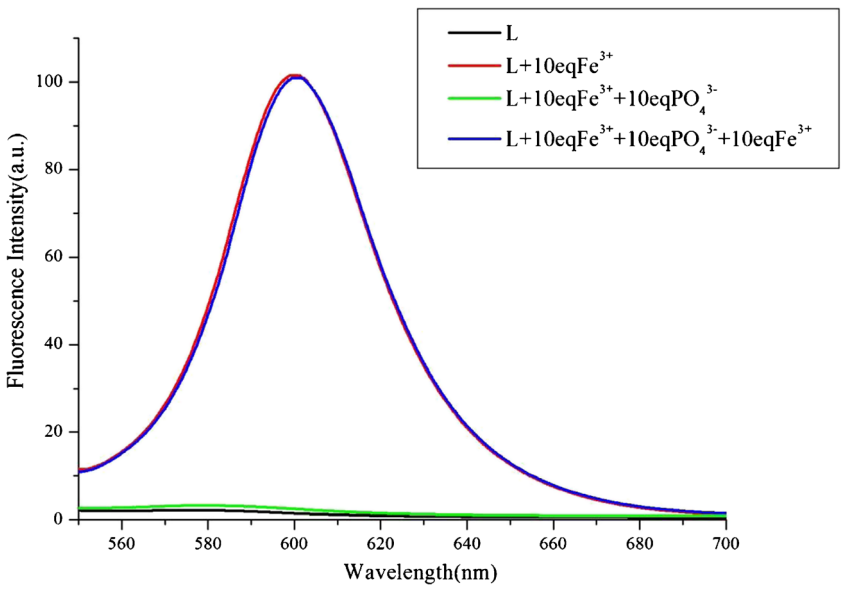

Fig. 7 Fluorescence intensity (at 600 nm) of **L** (10 μM) to Fe^{3+} in Tris-HCl buffer solution (2.5 mM, pH = 7.0). (1) Baseline: 10 μM **L** only; (2) *red line*: 10 μM **L** with 10 equiv. Fe^{3+}; (3) *green line*: 10 μM **L** with 10 equiv. Fe^{3+} and then addition of 10 equiv. K_3PO_4;(4) *blue line*: 10 μM **L** with 10 equiv. Fe^{3+} and 10 equiv. K_3PO_4, then addition of 10 equiv.Fe^{3+} (λ_{ex} = 520 nm, slit =5 nm)

Scheme 2 Possible sensing mechanism of **L** with Fe^{3+}

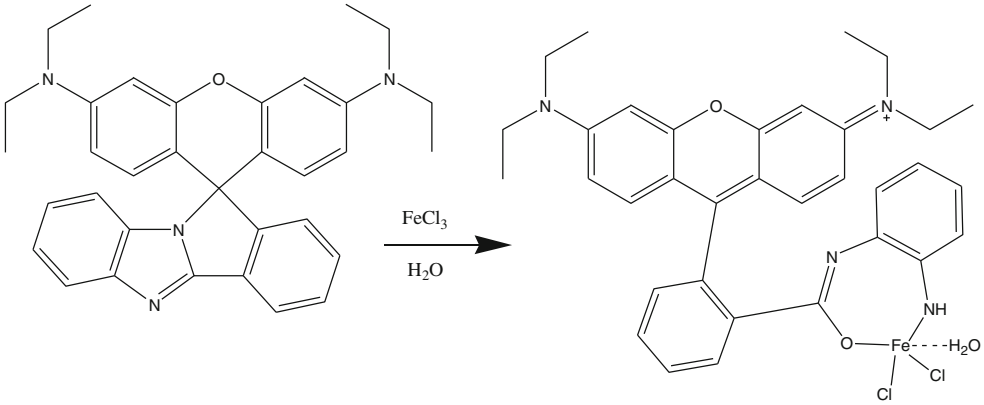

very low interference with the detection of Fe^{3+}. Moreover, the competitive experiments also confirmed that the background metal ions showed very low interference with the detection of Fe^{3+} in water solution. The fluorescence response of **L** toward Fe^{3+} in the presence of various coexistent anions was also investigated, and it was gratifying to notice that all the tested anions had low interference (Fig. 5).

To further investigate the interaction of chemosensor **L** with Fe^{3+}, a fluorescence titration experiment was conducted. As shown in Fig. S5, the fluorescence intensity of **L** was enhanced with the increasing concentration of Fe^{3+}. Moreover, the time-dependence fluorescence of probe **L** was also evaluated in the presence of Fe^{3+} ions (Fig. 6). The kinetics of fluorescence enhancement at 600 nm by the probe **L** were recorded, and the results indicated that the recognizing event could be completed in 10 s (T = 25 °C). These results also demonstrated that compound **L** was a selectivity and rapidly sensor for Fe^{3+} over various other metal ions.

In order to investigate the influence of the different acid concentration on the spectra of **L** and found a suitable pH span in which **L** could selectively detect Fe^{3+} efficiently, the acid titration experiments were performed. As shown in Fig. S6, the fluorescent titration curve of free sensor **L** in Tris-HCl buffer solution did not show obvious characteristic color of rhodamine between pH 5.8 and 7.4, suggesting that spirolactam tautomer of **L** was insensitive to the pH changes in this range. However, the addition of Fe^{3+} led to the fluorescence enhancement over a comparatively wide pH range (5.8–7.4), which was attributed to opening of the rhodamine ring. Consequently, **L** might be used to detect Fe^{3+} in approximate physiological conditions. Generally, the detection limit of the fluorescence sensor was one of the most important and useful application. Under optimal conditions, the linear response for the fluorescence intensity response was between 0 and 1 μM (Fig. S7), and the detection limit of Fe^{3+} was measured to be 2.74 μM.

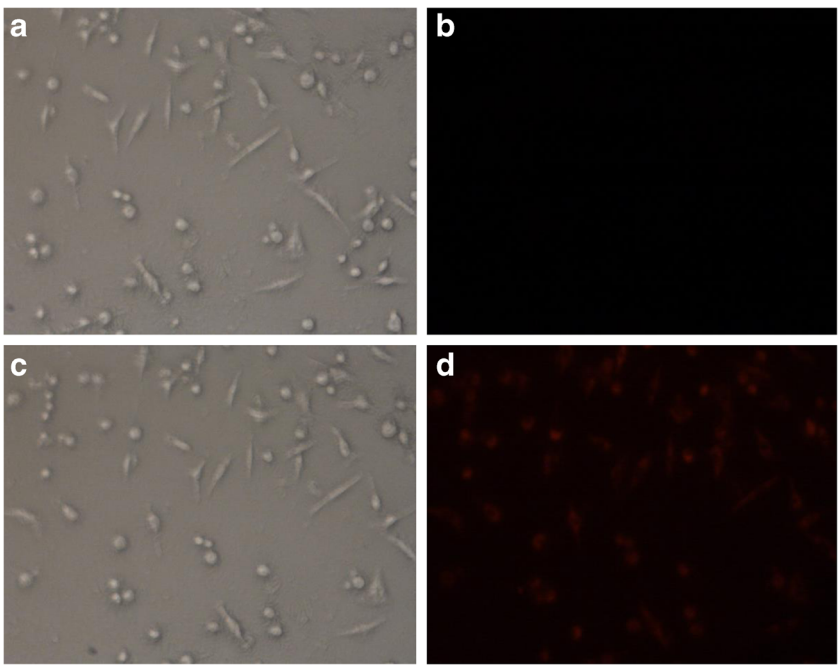

Fig. 8 Fluorescence images of Fe^{3+} in MGC-803 cells with 10 μM solution of **L** in H_2O for 30 min at 37 °C, bright-field transmission images (a, c) and fluorescence images(b, d) of MGC-803 cells incubated with 0 μM, 10 μM of Fe^{3+} for 15 min, respectively

Mechanism

Further, it was of great interest to investigate the reversible binding nature of the sensor (shown in Fig. 7). Upon addition of 10 equiv. K_3PO_4 to the solution of 10 μM **L** with Fe^{3+} (10 equiv.), the fluorescence intensity at 600 nm was quenched (green line) due to the competitive binding of Fe^{3+} from **L** by K_3PO_4. Further addition of 10 equiv. Fe^{3+} could recover the strong fluorescence again (blue line). These indicated that the coordination of compound **L** with Fe^{3+} was reversible. According to the 1:1 stoichiometry of the Fe^{3+} to **L** in the complex (Fig.S4), a possible sensing mechanism was postulated (Scheme 2). It was supported by the HR-MS spectra. A directly evidence was obtained by comparing the HR-MS of **L** (Fig. S3) and **L** + Fe^{3+} (Fig. S8) in Tris-HCl solution (2.5 mM, pH = 7.0). An unique peak at m/z = 658.9 corresponding to $[\mathbf{1}+ Fe^{3+}+H_2O + 2Cl^-]^+$ was clearly observed when 1 equiv. of $FeCl_3$ was added to **L**, whereas **L** without Fe^{3+} exhibited peaks only at m/z 515.3 which corresponded to $[\mathbf{L} + H]^+$. Moerover, the peaks at m/z = 533.1 and m/z = 555.1 were considered as $[\mathbf{1}+ H_2O]^+$ and $[\mathbf{1}+ K]^+$.

Bioimaging Application of Compound L in MGC-803 Cells

To further assess the potential applications of the probe in living cells, fluorescent imaging in MGC-803 cells was monitored by fluorescence microscopy. As shown in Fig. 8b, very weak fluorescence of **L** inside the living MGC-803 cells was observed. After washing with water twice, 10 μM of Fe^{3+} was then supplemented to the cells. After incubated at 37 °C for 15 min, a significant increase in the fluorescence from the intracellular area was observed (Fig. 8d). A bright field transmission image of cells with Fe^{3+} and **L** confirmed that the cells were viable throughout the imaging experiments (Fig. 8a and c). These results indicated that **L** might be useful for detecting Fe^{3+} in biological samples.

Conclusion

In summary, an efficient rhodamine-based fluorescent Chemosensor **L** was synthesized. The probe exhibited selectivity and sensitivity in Tris-HCl buffer solution (2.5 mM, pH = 7.0) with dramatic enhanced fluorescence intensities. The significant changes in the fluorescence color could be used for naked-eye detection. **L** might be used to detect Fe^{3+} in some environmental regions in a wide pH range with a detection limit up to 2.74 μM. Moreover, it was applied for imaging in MGC803 cells to confirm that it could be used as a fluorescent sensor for monitoring Fe^{3+} in living cells.

Acknowledgments This work was supported by the National Science Foundation of China (Nos. 21572209) and Program for New Century Excellent Talents in University (NCET-11- 0950).

References

1. James P, Raoul K (2005) Analyst 130:528–533
2. Wang L, Ye Y, Zhong S, Zhao Y (2009) Chin Chem Lett 20:58–61
3. Meneghini R (1997) Free Radic Biol Med 23:783–790
4. Wang L, Ye Y, Zhong S, Zhang D, Zhao Y (2009) Chem J Chinese U 30:493–496
5. Eisenstein RS (2000) Annu Rev Nutr 20:627–630
6. Rouault TA (2006) Nat Chem Biol 2:406–409
7. Brugnara C (2003) Clin Chem 49:1573–1479
8. Burdo JR, Connor JR (2003) *Brain iron uptake and homeostatic mechanisms*: *an overview*. Biometals 16:63–75
9. H. N. Kim, M. H. Lee, H. J. Kim, J. S. Kim. J. Yoon, Chem Soc Rev 37 (2008) 1465–1476.
10. Tumambac GE, Rosencrance CM, Wolf C (2004) Tetrahedron 60: 11293–11297
11. Beija M, Afonso CAM, Martinho JMG (2009) Chem Soc Rev 38: 2410–2418
12. Hu Z, Feng Y, Huang H, Ding L, Wang X, Lin C, Li M, Ma C (2011) Sensors Actuators B 156:428–433
13. Dylan WD, Emily LQ (2008) J C Christopher *Nat Chem Bio* 4: 168–175
14. Chen X, Hong H, Han R, Zhang D, Ye Y, Zhao Y (2012) *J Fluoresc* 22:789–794
15. Shi W, Ma HM (2012) Chem Commun 48:8732–8744
16. Lin W, Long L, Yuan L, Cao Z, Feng J (2009) *Anal Chim Acta* 634: 262–266
17. Yin W, Cui H, Yang Z, Li C, She M, Yin B, Li J, Zhao G, Shi Z (2011) Sensors Actuators B 157:675–680
18. Yang Z, She M, Yin B, Cui J, Zhang Y, Sun W, Li J, Shi Z (2012) J Organomet Chem 77:1143–1147
19. Moon K, Yang Y, Ji S, Tae J (2010) Tetrahedron Lett 51:3290–3293
20. Hu Z, Feng Y, Huang H, Ding L, Wang X, Lin C, Li M, Ma C (2011) Sensors Actuators B 156:428–432
21. Zhang D, Zou R, Wang M, Chai M, Wang X, Ye Y, Zhao Y (2013) *J Fluoresc* 23:13–19
22. Xue ZW, Chen ML, Chen JM, Han JH, Han SF (2014) RSC Adv 4: 374–378
23. Zheng H, Shang GQ, Yang SY, Gao X, *Org* JGX (2008) Lett 10: 2357–2360
24. Huang CY (1982) Methods Enzymol 87:509–525